0026-895X/96/051388-13$3.00/0

MOLECULAR PHARMACOLOGY, 50:1388–1400 (1996).

Distinct Effects of Mutations in Transmembrane Segment IVS6 on Block of L-Type Calcium Channels by Structurally Similar Phenylalkylamines

BARRY D. JOHNSON, GREGORY H. HOCKERMAN, TODD SCHEUER, and WILLIAM A. CATTERALL

Department of Pharmacology, University of Washington School of Medicine, Seattle, Washington 98195-7280

Received May 20, 1996; Accepted July 25, 1996

SUMMARY

The phenylalkylamines (−)-D888, verapamil, and D600, cause voltage- and use-dependent block of L-type Ca^{2+} channels and differ from each other only in the number of methoxy groups on each of their two terminal phenyl rings. To study the effects of mutations in the phenylalkylamine receptor site on block by these drugs, wild-type and mutant Ca^{2+} channels were transiently expressed in the tsA-201 clone of human embryonic kidney 293 cells. The combined mutations Y1463A, A1467S, and I1470A (mutant YAI) in transmembrane segment S6 of domain IV of the α_{1C} subunit disrupted block by all three phenylalkylamines. Surprisingly, although this mutation reduced both resting block at −60 mV and depolarized block at +10 mV by (−)-D888, resting and depolarized block by verapamil and D600 were relatively unaffected. In contrast, for all three drugs, use-dependent block during repetitive stimulations was sharply reduced, and the rate of recovery from depolarized block was accelerated for YAI channels. Thus, the effects of the YAI mutation on apparent affinity were specific to (−)-D888, whereas effects on the kinetics of block were observed for all three drugs. Additional experiments with substitution of phenylalanine for Y1463 suggested that (−)-D888 affinity is specifically sensitive to removal of the hydroxyl group of Y1463, whereas effects on the kinetics of block by all three phenylalkylamines require larger molecular changes, perhaps related to residue size and hydrophobicity. Analysis of the data using a state-dependent model of drug block suggests that these kinetic differences are caused by both changes in drug access to the receptor site and affinity for binding to the inactivated state of the channel. The different effects of the YAI mutations on the actions of (−)-D888, verapamil, and D600 indicate that these residues interact differently with these closely related drugs.

The phenylalkylamines potently block L-type Ca^{2+} channels and are used clinically to treat cardiac arrhythmias, hypertension, and angina pectoris (1), conditions in which L-type Ca^{2+} channels in cardiac and smooth muscle play a central role. The biochemically isolated L-type Ca^{2+} channel from skeletal muscle is a multimeric complex consisting of $\alpha1$, $\alpha2$, β, γ, and δ subunits, and specific isoforms of the $\alpha1$, $\alpha2\delta$, and β subunits are expressed in the heart (2–4). The $\alpha1$ subunit is homologous to other members of the voltage-gated ion channel family and consists of four homologous domains (I–IV), each of which contains six putative transmembrane segments (S1–S6). The $\alpha1$ subunit is the principal functional constituent of the channel, containing the machinery for voltage-dependent gating, ion conductance, and block by calcium channel antagonists (2).

Phenylalkylamines block calcium channels in a voltage- and use-dependent manner. Low affinity block is observed at the resting potential, but block is much more effective during trains of depolarizing pulses or single long depolarizations (5). Tertiary phenylalkylamines exist in charged and neutral forms at physiological pH. A quaternary, permanently charged phenylalkylamine, D890, blocks calcium channels only from the intracellular side in most tissues, suggesting that the charged form of these drugs must reach their binding site from inside the cell (6). Most of the characteristics of drug block can be explained by a model in which phenylalkylamines bind to a site in the ion channel pore that is modulated by the conformation of the channel, as has been proposed for local anesthetic block of Na^+ channels (7). Block at this site is strongly voltage dependent, suggesting that it is in the membrane field, and block is increased by repetitive depolarizations.

Photoaffinity labeling of the $\alpha1$ subunit of purified skeletal muscle L-type Ca^{2+} channels with the high affinity phenylalkylamine LU49888 (8) resulted in specific derivatization of a peptide containing transmembrane segment IVS6 (9).

This work was supported by National Institutes of Health Research Grant P01-HL44948 (W.A.C.), a National Institutes of Health Postdoctoral Research Fellowship (G.H.H.), and a Muscular Dystrophy Association Postdoctoral Research Fellowship (B.D.J.).

ABBREVIATIONS: I_{Ba}, Ba^{2+} current; EGTA, ethylene glycol bis(β-aminoethyl ether)-*N*,*N*,*N*′,*N*′-tetraacetic acid; HEPES, 4-(2-hydroxyethyl)-1-piperazineethanesulfonic acid

Scanning mutagenesis of transmembrane segment IVS6 identified three amino acid substitutions [Y1463 to alanine (Y1463A), A1467 to serine (A1467S), and I1470 to alanine (I1470A)] that disrupted channel block by the high affinity phenylalkylamine (−)-D888 (desmethoxyverapamil) (10). A channel containing all three mutations was >100-fold less sensitive to block by (−)-D888, similar to the phenylalkylamine-insensitive N-type Ca^{2+} channel. The reversal potential for ion conductance through the open channel was altered, suggesting that channel selectivity was also affected by these mutations. Studies using chimeras formed between α1 subunits of L-type and non-L-type Ca^{2+} channels (11, 12) also indicate that transmembrane segment IVS6 contains the primary molecular determinants of the difference in phenylalkylamine sensitivity.

We extended our analysis of the pharmacological effects of mutations at these sites by examining tonic block by the lower affinity phenylalkylamines, verapamil, and methoxyverapamil (D600), analyzing the voltage- and time-dependent properties of use-dependent block by these compounds, and comparing the effects of substitution of other amino acids for the most critical amino acid residue in this segment, Y1463. Surprisingly, these mutations had different effects on block by verapamil and its closely related derivatives (−)-D888 and D600, each of which differs from verapamil by only one methoxy group. The common and divergent effects of mutations on block by these drugs begin to provide a molecular picture of how these drugs interact with the calcium channel.

Materials and Methods

Molecular biology. All mutations were constructed using oligonucleotide-directed mutagenesis as described previously (10, 13). The 1.5-kb *Esp*I fragment of the α1CII subunit of rat brain Ca^{2+} channels (14) was subcloned into bacteriophage M13 mp19 for recovery of single-stranded DNA template. Mutations were inserted into full-length channel constructs in the expression vector Zem229 (Dr. Eileen Mulvihill, Zymogenetics, Seattle, WA) using the 272-bp *Dra*III fragment (nucleotides 5095–5366). All mutations were confirmed by DNA sequencing.

Cell culture and expression of channel subunits. WT and mutant α1CII channel subunits were coexpressed with β1b subunits (15) in vector pMT-2 (Genetics Institute, Cambridge, MA) and $\alpha 2\delta 1$ subunits (16) in vector Zem 228 (Dr. Eileen Mulvihill, Zymogenetics) as well as with a vector encoding CD8 (EBO-pCD-Leu2, American Type Culture Collection, Rockville, MD). These cDNAs were transfected into tsA201 cells through $CaPO_4$ precipitation essentially as described previously (17). tsA201 cells, a subclone of the human embryonic kidney 293 cell line, which expresses simian virus 40 T antigen (a gift of Dr. Robert Dubridge, Cell Genesis, Foster City, CA), were maintained in a monolayer culture in Dulbecco's modified Eagle's medium/F-12 medium (GIBCO BRL, Baltimore, MD) supplemented with 10% fetal bovine serum (Hyclone, Logan, UT) and incubated at 37° in 10% CO_2. Cultures in 35-mm tissue culture dishes that were 75% confluent were transfected with a total of 4 μg of DNA consisting of an equimolar ratio of the three channel subunit cDNAs and 0.8 μg of CD8 cDNA. After the addition of $CaPO_4$-DNA, cells were incubated overnight at 37° in 5% CO2. Twenty hours after transfection, the cells were removed from culture dishes with the use of 2 mM EDTA in phosphate-buffered saline and replated at low density for electrophysiological analysis. Transfectants were recognized by labeling with fluorescent anti-CD8 antibody (phycoerythrin-labeled anti-CD8; Sigma Chemical, St. Louis, MO) using an epifluorescence microscope (rhodamine filter; Nikon Diaphot).

Electrophysiology. I_{Ba} through L-type Ca^{2+} channels was recorded using the whole-cell configuration of the patch-clamp technique. Patch electrodes were pulled from VWR micropipettes and fire-polished to produce an inner tip diameter of 4–6 μm. Currents were recorded using a List EPC-7 patch-clamp amplifier and filtered at 2 kHz (eight-pole Bessel filter, −3 dB). Voltage pulses were applied and data were acquired using Fastlab software (Indec Systems, Capitola, CA). Currents have been corrected for linear leak and capacitance using an on-line P/4 subtraction paradigm. The phenylalkylamines (−)-D888, verapamil, and D600 (Knoll, Ludwigshafen, Germany) were applied to cells by the addition of 0.2 ml of 6× concentrated solution to a 1-ml bath. The bath saline contained 150 mM Tris, 2 mM $MgCl_2$, and 10 mM $BaCl_2$. The intracellular saline contained 130 mM *N*-methyl-D-glucamine, 10 mM EGTA, 60 mM HEPES, 2 mM MgATP, and 1 mM $MgCl_2$. pH of each solution was adjusted to 7.3 with methanesulfonic acid. All experiments were performed at room temperature (20–23°). No nonlinear outward currents were detected under these conditions. The voltage dependence of inactivation for mutant channels was determined using 5-sec prepulses and fitting with a Boltzmann distribution as described previously (10).

State-dependent model of drug block. Channel distributions between states were calculated numerically with a time increment of 100 μsec. Rate constants (in sec^{-1}) between channel states in the absence of drug are summarized in Table 1 for +10 mV (depolarized) and −60 mV (resting). Transitions rates between drug-bound states were determined by fitting the resting channel block (Fig. 2B), the magnitude of depolarization-induced drug block (Fig. 2C), and time course of recovery from depolarized drug block (Fig. 9B) to the mean values shown in the figures. The time course of resting channel drug block (i.e., C–CB) was not determined with adequate resolution in these experiments, so the rates were arbitrarily set to values slower than block of other channel states. To simplify the model and because they were not determined independently, rates of drug block and unblock were set at the same for states I_1 and I_2 (e.g., I_1–I_1B = I_2–I_2B), making I_1B–I_2B and I_2B–I_1B transitions independent of drug concentration and equal to I_1–I_2 and I_2–I_1, respectively. OB–I_1B was assumed to be independent of drug concentration and was set to 0.3 at +10 mV and 0.01 at −60 mV. OB–CB was also assumed to be independent of drug concentration and was set to 2.2 at +10 mV from results on WT channels in the absence of drug and to 0.9 at −60 mV. To maintain microscopic reversibility (conservation of energy) in this model, two transition rates were calculated as a function of the other transition rates: CB–OB = (C–O × O–OB × CB–C × OB–CB)/(C–CB × OB–O × O–C) and I_1B–OB = (I_1–O × O–OB × I_1B–I_1 × OB–I_1B)/(O–I_1 × I_1–I_1B × OB–O). The remaining transitions rates and the resulting K_d values are summarized in Table 2.

Results

Voltage-dependent tonic block of WT Ca^{2+} channels by (−)-D888, verapamil, and D600. Although the pharmacological properties of verapamil, (−)-D888, and D600 are

TABLE 1

Rate constants for transitions between channel states

Ca^{2+} channel activation, inactivation, deactivation, and recovery from a 1-sec inactivating depolarization measured in control conditions saline were fit with the model shown in Fig. 8D (*inset*). Channels were depolarized from a resting potential of −60 mV to +10 mV for 1 sec. The behavior of the model using these rate constants is shown in Fig. 8A as solid lines superimposed on the actual data as either a dashed line (Fig. 8A) or data points (Fig. 6B, *inset*).

	C–O	O–C	O–I_1	I_1–O	I_1–I_2	I_2–I_1
			sec^{-1}			
+10 mV	220	2.2	0.8	1	0.8	0.001
−60 mV	1	1249	0.8	3.3	0.01	0.09

C, closed; O, open; I_1 and I_2, inactivated states.

significantly different (18), their structures are very similar (Fig. 1A). Our previous studies (10) implicated three amino acid residues in transmembrane segment IVS6 of the Ca^{2+} channel α1C subunit in high affinity binding of (−)-D888 (Y1463, A1467, I1470; Fig. 1B). In the current experiments, phenylalkylamine block of L-type Ca^{2+} channels was studied by recording inward I_{Ba} in tsA201 cells transiently expressing cDNAs encoding the α1C, β1b, and $\alpha 2\delta$ subunits. Fig. 1, C–E (*left*). shows the decrease in size and change in time course of WT I_{Ba} in individual cells in response to a range of concentrations of the phenylalkylamines (−)-D888, verapamil, and D600. After the beginning of whole-cell recording, I_{Ba} amplitude was monitored until it was stable with the use of 100-msec test depolarizations to +10 mV applied every 15 sec from a holding potential of −60 mV. Drugs were then introduced into the bath at the indicated concentration, and currents were monitored until block reached equilibrium. Because channels activate infrequently in this protocol, drug block under these conditions reflects steady state binding to the mixture of closed and closed/inactivated states present at −60 mV, and we refer to this as "tonic block of resting channels" or "resting block." The extent of resting block was characterized by measuring the peak I_{Ba} early during the 1-sec test depolarization to +10 mV. Under these conditions, the three phenylalkylamines differed in potency. Most of the peak I_{Ba} was blocked by 500 nM (−)-D888 (Fig. 1C), whereas less than half of the current was blocked by the same concentration of verapamil (Fig. 1D) or D600 (Fig. 1E). Assuming a 1:1 binding reaction (Fig. 2A), IC_{50} values for tonic block at the holding potential of −60 mV were 50 ± 5 nM for (−)-D888, 7 ± 2 μM for verapamil, and 8 ± 1 μM for D600 (Fig. 2B, *open bars*).

Phenylalkylamines increased the rate of decay of the I_{Ba} during the depolarizing pulse (Fig. 1, C–E). This dose-dependent increase in decay rate is most striking for verapamil. The decay time course is caused by the development of drug block during the depolarization (5) and is characteristic of compounds that block the open and inactivated states of Ca^{2+} channels that are present at depolarized potentials more potently than the resting state present at −60 mV. If drug block reaches a steady state during the pulse, the degree of block reached at the end of the pulse represents equilibrium block at the test potential and drug concentration. We refer to this as "tonic block of depolarized channels" or "depolarized block." To estimate the affinity of channels for drug at a depolarized potential, the reductions in current relative to controls at the end of 1-sec depolarizations to +10 mV (e.g., Fig. 1) were measured and fit assuming a 1:1 binding reaction. For verapamil, the IC_{50} value for block at +10 mV (331 ± 153 nM) was 20-fold lower than that for resting block at −60 mV (Fig. 2A). The IC_{50} values for (−)-D888 and D600 at +10 mV were 10.7 ± 2.6 and 782 ± 255 nM, respectively, 4.7-fold and 10-fold lower than at the resting potential (Fig. 2, B and C). These IC_{50} values for block of Ca^{2+} channels measured at the end of 1-sec depolarizing pulses to +10 mV are overestimates because the block has not fully reached steady state in 1 sec for all drug concentrations (Fig. 1, C–E). The estimates are most accurate for verapamil because of its rapid blocking kinetics (Fig. 1D). The lower ratios of drug block at −60 and +10 mV for the more slowly blocking drugs (D888 and D600) may be influenced by underestimates of steady state block at the end of 1-sec depolarizing pulses. Development of voltage-dependent inactivation during longer depolarizations makes an exact measure of depolarized block for these drugs difficult because the current amplitude is reduced to <10% after 5 sec. However, experiments using the slowest blocking drug, D600, indicate that IC_{50} values measured at 1 sec are overestimated by no more than 4-fold compared with measurements taken at the end of 5-sec depolarizations to +10 mV.

Effect of mutation YAI on voltage-dependent tonic block. Mutation of three hydrophobic residues in transmembrane segment IVS6, Y1463A, A1467S, and I1470A (*YAI*, Fig. 1B) resulted in channels with a 100-fold increase in the IC_{50} value for tonic block of resting Ca^{2+} channels by (−)-D888 from 50 nM to 5 μM (Figs. 1 and 2) (10). Surprisingly, mutant YAI channels had only a 1.6-fold increase in IC_{50} for block of peak I_{Ba} by D600 from 8 to 13 μM, and the affinity for block by verapamil was unchanged (6.7 ± 2.0 to 6.0 ± 1.5 μM, Fig. 2B). In fact, the IC_{50} values for resting block of the mutant channel by all three drugs at −60 mV were similar with IC_{50} values ranging from 5 to 13 μM. In addition, the range of IC_{50} values for depolarized block by these three drugs was 104–670 nM for mutant YAI, whereas they differed by 73-fold in WT channels (Fig. 2C). Thus, mutation of these three residues selectively reduces the binding of the high affinity blocker (−)-D888 with relatively little effect on binding of the lower affinity blockers verapamil and D600. This mutation therefore makes the affinities for resting and depolarized block of the mutant channel by all three drugs similar to each other.

Because pure (−)-enantiomers of verapamil and D600 are more potent Ca^{2+} channel blockers (19) than the racemic compounds, the effect of mutant YAI on block by (−)-verapamil was also tested. The mean IC_{50} values at −60 mV for (−)-verapamil block of WT and YAI channels were 1.0 ± 0.2 and 1.2 ± 0.3 μM (n = 5), respectively. Although (−)-verapamil produced significantly more potent block than the racemic mixture, it did not reveal a larger difference between WT and YAI channels.

Effects of mutation of the individual amino acid residues composing YAI on voltage-dependent tonic block. To determine whether the effects of mutant YAI could be assigned to one of its component amino acids, channel constructs in which each of the individual amino acids had been mutated were used to compare the blocking characteristics of (−)-D888 and verapamil. Mutation of the single amino acid residues increased the IC_{50} for tonic block by (−)-D888 by 6–12-fold in comparison to the 100-fold increase for the combined YAI mutation (Fig. 3A). In contrast, the effect of each individual mutation on block of depolarized channels by (−)-D888 was nearly as great as the effect of mutating all three amino acids (Fig. 3B). As expected from the lack of effect of the YAI mutation on resting or depolarized block by verapamil, mutation of individual amino acids was also ineffective (Fig. 3, A and B).

Our previous study showed that mutation Y1463A in combination with either of the other two mutations (YA or YI) could cause the full disruption of high affinity (−)-D888 block observed with mutant YAI, whereas the AI combination could not (10). This indicated that Y1463 plays a central role in disruption of block by (−)-D888. To more extensively explore the structural requirements for the interaction of Y1463 with the phenylalkylamines, mutants Y1463T and

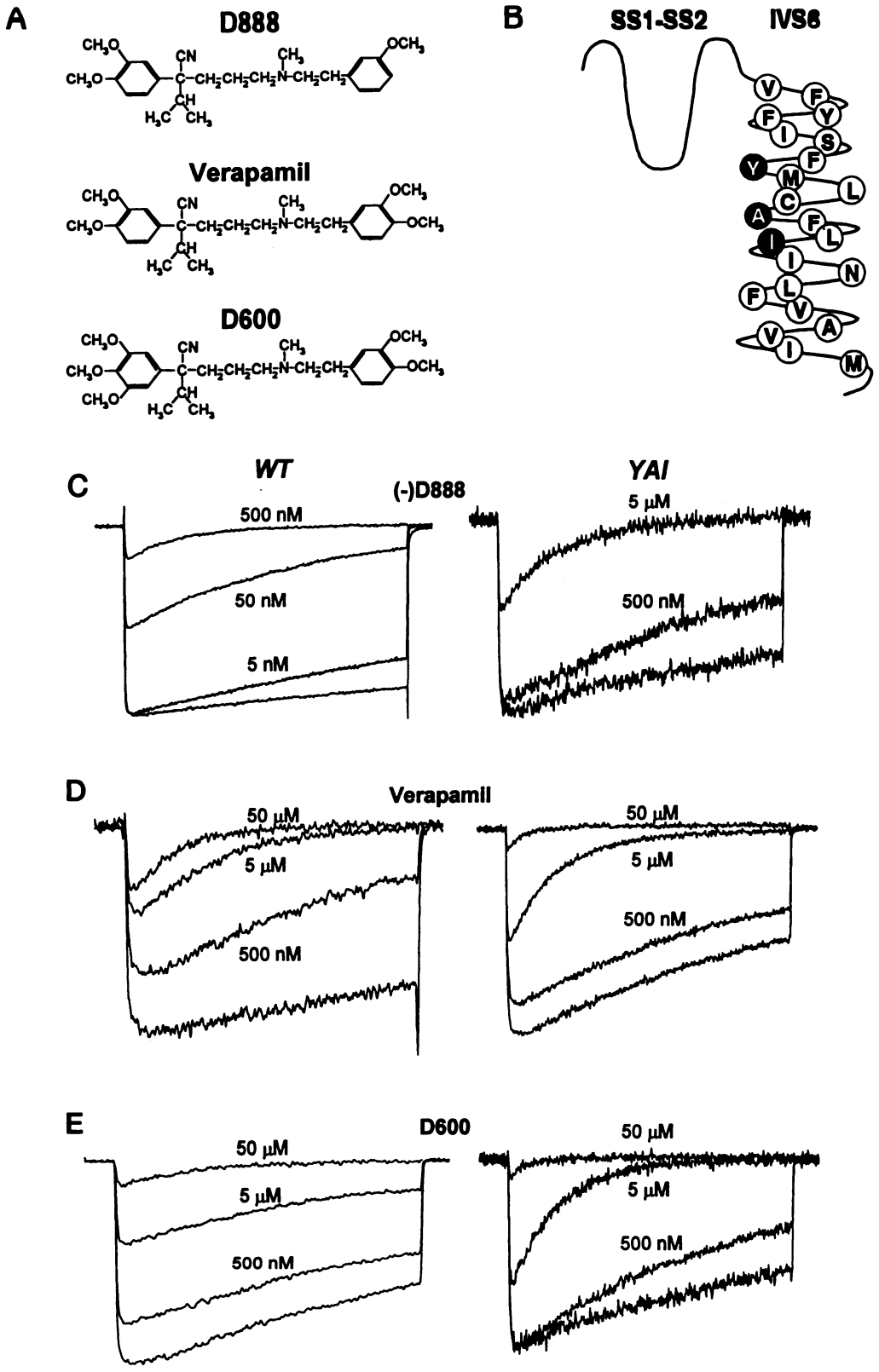

Fig. 1. Phenylalkylamine block of WT and YAI mutant L-type Ca^{2+} channels. A, Structures of D888, verapamil, and D600. B, Model of phenylalkylamine interaction with the Ca^{2+} channel. The residues in the sixth transmembrane segment of homologous domain four (IVS6) of the L-type Ca^{2+} channel are shown in an α helical arrangement with Y1463 facing the lumen of the pore. C, D, and E, Phenylalkylamines (C) (−)-D888, (D) verapamil, and (E) D600 applied at the concentrations shown to tsA201 cells expressing WT or YAI mutant α1C calcium channel subunits along with β1b and α2δ subunits. In the YAI mutant α1C subunit, three amino acids in IVS6 have been mutated: Y1463A, A1467S, and I1470A. The currents shown in each panel were obtained from a single cell in which the indicated drug was applied at increasing concentrations. They were elicited by 1-sec depolarizations to +10 mV. The holding potential was −60 mV for all experiments. Currents in control have been scaled to similar peak amplitudes. Actual amplitudes ranged from 120 pA to 1 nA. During drug application, I_{Ba} amplitude in response to 100-msec depolarizations to +10 mV applied every 15 sec was monitored until current reduction reached a steady state.

Y1463F were constructed. The substitution of phenylalanine for tyrosine removed only the phenolic hydroxyl at this position, whereas substitution of threonine removed the large phenyl ring, leaving a smaller side chain containing a hydroxyl group on an aliphatic rather than an aromatic side chain. Like the YAI and Y1463A mutations, these two mutations had distinct effects on block by (−)-D888 and verapamil. The increase in the IC_{50} for resting block by (−)-D888 at −60 mV for the Y1463F and Y1463T mutations was somewhat greater than the increase for Y1463A (Fig. 3C). Both Y1463F and Y1463T also substantially increased the IC_{50} for block of depolarized Ca^{2+} channels by (−)-D888 (Fig. 3D).

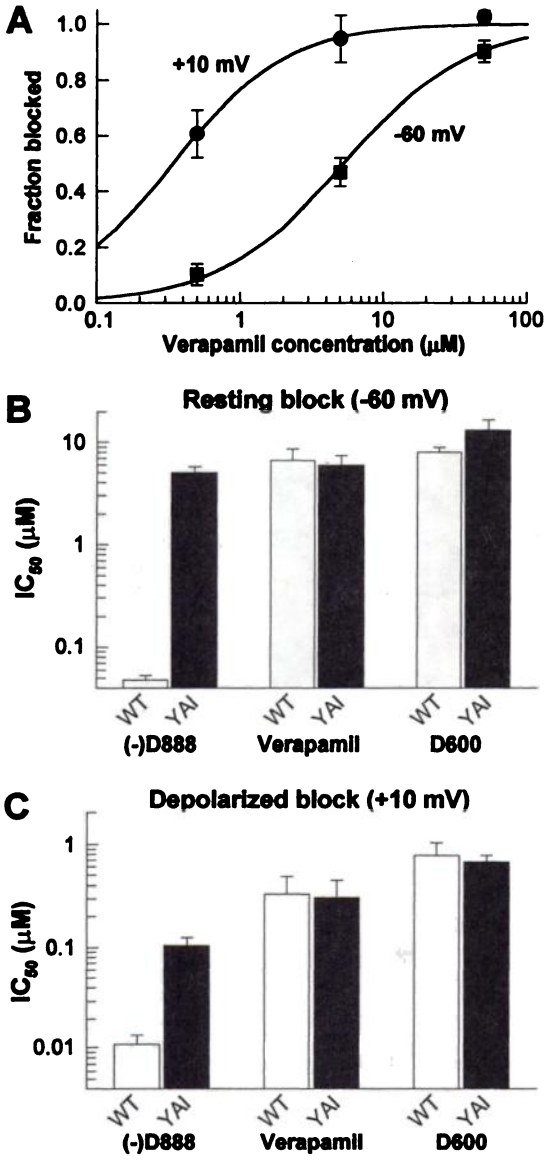

Fig. 2. Comparison of tonic and depolarized channel block. Block of peak current and current measured at the end of 1-sec depolarizations to +10 mV were used to estimate resting and depolarized channel affinities, respectively. A, Resting and depolarized block of WT channel by 500 nM, 5 μM, and 50 μM verapamil (n = 5–8). *Solid lines*, fits to the data with the equation $1/(1 + ([IC_{50}/[drug]])$, which gave a resting IC_{50} value of 5.3 μM and a depolarized IC_{50} value of 339 nM. Block of WT and YAI channels by drug concentrations from 50 nM to 50 μM was fit with the equation above to give the resting block (B) and depolarized block (C) results shown (n = 8–38). Note the 10-fold reduction in the *ordinate scale* of C.

These results indicate that the phenolic hydroxyl of Y1463, which is the only structural change in Y1463F, has a surprisingly strong effect on (−)-D888 affinity for resting Ca^{2+} channels, and this effect is not replaced by the hydroxyl of a substituted threonine residue. In contrast to the results with (−)-D888, IC_{50} values for resting or depolarized block of Y1463A, Y1463F, and Y1463T by verapamil were not significantly different from those of WT channels, and block of depolarized Y1463F and Y1463T channels showed small changes that barely reached statistical significance (Fig. 3, C and D). Overall, these results indicate that residues Y1463, A1467, and I1470 interact strongly with (−)-D888 during steady state block of resting and open/inactivated channels but much less strongly with verapamil or D600.

Voltage-dependent phenylalkylamine block of Ca^{2+} channels is influenced by the inactivation mechanism of the L-type Ca^{2+} channel (5), and effects on inactivation might cause indirect effects on channel block. Although mutants YAI and Y1463A cause substantial positive shifts in the voltage dependence of inactivation (10), mutants A1467S, I1470A, Y1463F, and Y1463T do not affect the voltage dependence of inactivation ($V_{1/2}$ values were for WT channels: −17.7 mV, YAI: −9.3, Y1463A: −7.5, A1467S: −17.8, Y1463F: −19.2, I1470A: −22.8, Y1463T: −16.7). Because each of these mutants disrupted block by (−)-D888, the disruption of drug block by these mutations cannot be attributed to indirect effects on the voltage dependence of inactivation.

Use-dependent block by phenylalkylamines. During repetitive depolarizations, block by phenylalkylamines accumulates in a frequency- and voltage-dependent manner because additional drug binds during each depolarization and fails to unbind completely at the resting potential between depolarizations. Such use-dependent block is important for the clinical efficacy of these drugs. Use-dependent Ca^{2+} channel block by the three phenylalkylamines was compared in control and YAI mutant channels (Fig. 4). A 1-Hz train of twenty 100-msec depolarizations to +10 mV was applied both in the presence of 500 nM (−)-D888, 5 μM verapamil, or 5 μM D600 and in the absence of drug. These concentrations were chosen to compare use-dependent block of WT and YAI channels in the same concentration of drug, near the IC_{50} values at −60 mV for verapamil and D600 and halfway, on a logarithmic scale, between the IC_{50} values of WT and YAI mutant channels for (−)-D888. To correct for accumulation of voltage-dependent inactivation during the train in control, current measured in the presence of drug was divided by current measured in the absence of drug. This correction averaged 30% at the end of the 20-pulse train. Each drug produced use-dependent block in the WT channel, but it was more pronounced for (−)-D888 and D600 than for verapamil (Fig. 4). Less use-dependent block was observed in the YAI mutant channel for each drug. The large decrease in block of the YAI mutant by (−)-D888 (Fig. 4A) was expected due to the large difference between affinities of the WT and YAI mutant channels for block by the drug. However, verapamil and D600 showed far less use-dependent block of the YAI channel despite their similar affinities for resting or depolarized WT and YAI channels (Fig. 4B). The discrepancy between the small effects of the mutation on the steady state affinity for verapamil and D600 and the large effect on the amount of use-dependent block suggested that this combined mutation may significantly alter the kinetics of phenylalkylamine block during repetitive trains of depolarizations.

Information about rate constants for drug block of depolarized channels and recovery from block between pulses can by derived from the pulsewise reduction in current observed during use-dependent trains (20, 21). At least two exponential components were required to fit the time course of pulsewise current reduction, indicating that channels entered two different blocked states during depolarizations and that channels in these two states recovered with different rates between depolarizations. Block at +10 mV was calculated according to the following (see below): $D + R \rightarrow DR_F \rightarrow DR_S$.

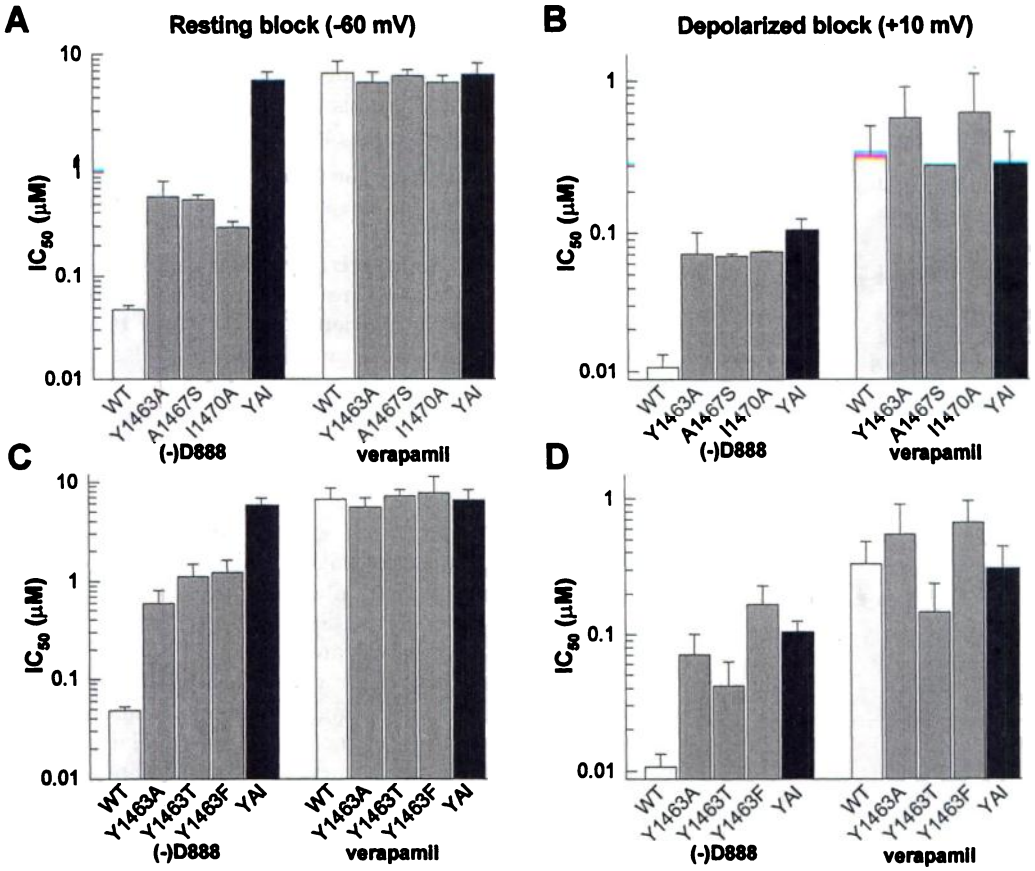

Fig. 3. Effect of individual amino acid substitutions on phenylalkylamine block. The individual mutations constituting the mutant YAI, Y1463A, A1467S, and I1470A and substitutions of phenylalanine (*F*) and threonine (*T*) for the tyrosine at position 1463 were characterized as described in previous legends. A and C, Mean IC_{50} value of peak current block measured from a holding potential of −60 mV (mean ± standard error, n = 5–12 for each mutant). B and D. Mean IC_{50} value of current block measured at the end of a 1-sec depolarization to +10 mV (n = 1–6 for each mutant). (−)-D888 was applied over a concentration range of 5 nM to 50 μM, and verapamil was applied over a range of 500 nM to 50 μM. Note the 10-fold reduction in the range of the *ordinate* in B and D.

Recovery −60 mV was calculated according to the following: $DR_S \rightarrow DR_F \rightarrow D + R$.

Fits to the data shown in Fig. 4 (*solid lines*) were derived from this empirical reaction scheme using the following parameters: (i) an apparent block rate at +10 mV (k_{app}), related to the decay of current during a depolarization (Fig. 1) in which drug (D) binds to the channel receptor site (R), and forms the DR_F and DR_S complexes, (ii) two time constants (τ_F, τ_S) for recovery at −60 mV from the fast (DR_F) and slow (DR_S) drug-bound states, respectively, and (iii) the fraction of channels entering the fast and slow blocked populations during the pulse (f_F and $1 - f_F$). This empirical analysis showed that YAI channels were blocked more slowly than WT channels by (−)-D888, at nearly the same rate by verapamil, and more rapidly by D600. The faster time constant of recovery (τ_F) was similar for all three drugs and for both channel types (≈500 msec). The slower time constant of recovery (τ_S) and the fraction of channels that recover rapidly (f_F) varied considerably for the three drugs. The slow recovery time constant (τ_S) varied between 12 and 20 sec for block of the WT channel by the three drugs (fastest in verapamil) and between 5 and 7 sec for YAI. The fraction of WT channels that recovered from depolarized block quickly was small for D888 and D600 (7%) and largest for verapamil (47%), whereas for YAI, the fraction of channels recovering from block with the faster time constant was 40–80% for all three drugs. The weak use-dependent block of YAI compared with WT channels results from both fewer channels entering the slowly recovering fraction of channels (state DR_S) and a faster time constant of recovery for channels that do enter. Thus, the number of channels entering the DR_S-blocked population during depolarizations and the rate at which these channels recover from drug block after repolarization differentiate among these drugs and mutants in their ability to produce use-dependent block. To obtain direct information about these rates, we examined the rate of onset of block during each depolarization to +10 mV and the rate of reversal of drug block on return to the resting membrane potential of −60 mV.

Rate of drug block during depolarizations. The rate at which channels become blocked during depolarizations was measured from the rate of decay of the current in the presence of drug as illustrated in Fig. 5 for D600. Current traces recorded in different drug concentrations were scaled to the same peak amplitude (Fig. 5A), showing the concentration-dependent increase in the rate of current decay during the pulse. To correct for the inactivation rate in control, each scaled trace was divided by the trace in control to give the time course of drug block during the pulse (Fig. 5B). This correction is only approximate because it does not account for inactivated channels that have also bound drug. Fig. 5B (*smooth lines*) shows single-exponential fits to the data that gave time constants of 7.7, 1.6, and 0.31 sec for 500 nM, 5 μM, and 50 μM D600, respectively. Rate constants determined by plotting data of this type versus concentration were 1.9×10^7 M^{-1} sec^{-1} for (−)-D888, 6.2×10^5 M^{-1} sec^{-1} for verapamil, and 3.2×10^5 M^{-1} sec^{-1} for D600. The rate constants for D600 block of WT channels are similar to those reported previously for block of cardiac channels (21).

Time courses of drug block were quite different in WT and mutant YAI channels, as indicated by the different rates of current decay at a given drug concentration (Fig. 1, C–E, compare *left* with *right*). This was particularly apparent for D600 (Fig. 1E). Mean time courses constructed as described

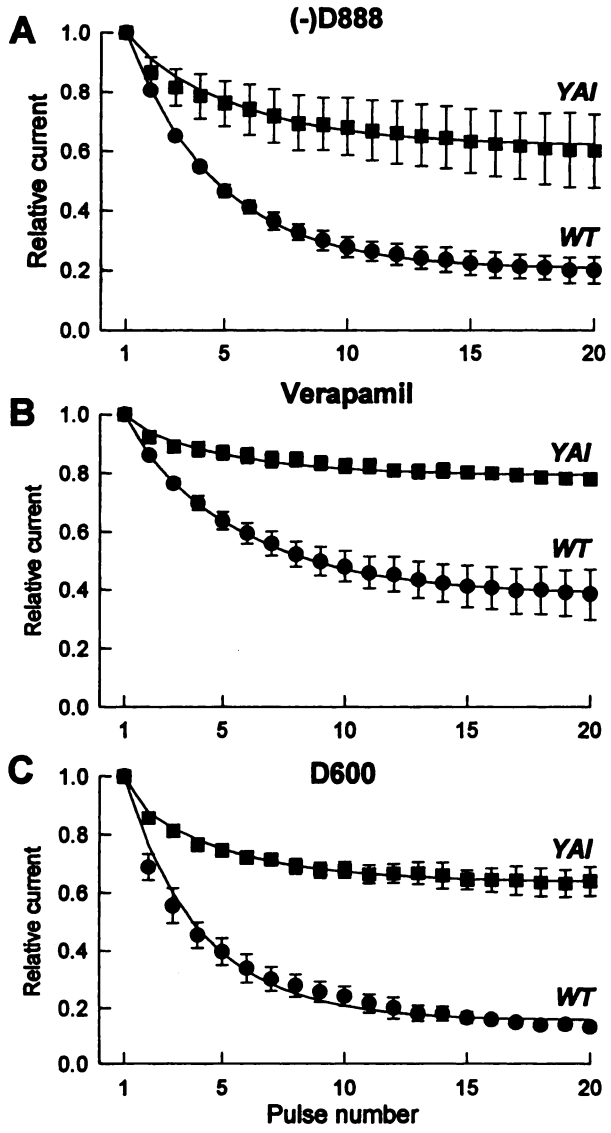

Fig. 4. Use-dependent block of WT and mutant L-type Ca^{2+} channel currents. A, 1-Hz train consisting of twenty 100-msec depolarizations to +10 mV was applied in the presence of (A) 500 nM (−)-D888, (B) 5 μM verapamil, or (C) 5 μM D600. Mean reduction in peak current (mean ± standard error) in each successive depolarizing pulse relative to that measured in the absence of drug (to correct for accumulation of voltage-dependent inactivation) is plotted against pulse number. Voltage-dependent inactivation at the end of the train measured in the absence of drug was 30% in both WT and YAI (n = 6) channels. *Solid lines*, fits to the data calculated from an apparent block rate (k_{app}), fast recovery time constant (τ_F), slow recovery time constant (τ_S), and fraction of channels recovering with the fast time constant (f_F). These values for D888 on WT channels were $k_{app} = 7 \times 10^6$ M^{-1} sec^{-1}, τ_F = 0.5 sec, τ_S = 18 sec, and f_F = 7%; for YAI, $k_{app} = 4 \times 10^6$, τ_F = 0.7, τ_S = 7, and f_F = 42%; for verapamil on WT channels, $k_{app} = 6.5 \times 10^5$, τ_F = 0.56, τ_S = 12, and f_F = 47%; for YAI, $k_{app} = 6.5 \times 10^5$, τ_F = 0.4, τ_S = 5, and f_F = 80%; for D600 on WT channels, $k_{app} = 6.3 \times 10^5$, τ_F = 0.6, τ_S = 20, and f_F = 7%; and for YAI, $k_{app} = 11 \times 10^5$, τ_F = 0.56, τ_S = 6, and f_F = 76%.

for WT and YAI channels in 5 μM D600 are shown in Fig. 5C. Single-exponential fits to these data (*smooth lines*) indicated that block of mutant YAI channels was more than twice as fast as block of WT channels. Mean apparent block rates (mean ± standard error, n = 3 or 4) are shown in Fig. 5D for each drug on both WT and YAI channels. The effect of the YAI mutation differed for the three phenylalkylamines. (−)-D888 blocked mutant YAI channels 8-fold more slowly than the WT channel, which is consistent with the large increase in IC_{50} for (−)-D888 block of the mutant channel. In contrast, block of YAI mutant channels by verapamil and D600 was 1.6- and 3.3-fold faster than for WT channels, respectively. Thus, the rates of block by the three drugs at +10 mV were dramatically different for the WT channel but were similar for the mutant YAI channel.

Recovery from depolarization-dependent block at −60 mV. For a direct measure of recovery from depolarized block, a 1-sec conditioning depolarization to +10 mV was applied. Recovery from block induced by that pulse was measured during an interval of variable duration at −60 mV followed by a 100-msec test pulse to +10 mV (Fig. 6). In the absence of drug, 41% of the channels inactivate in response to the 1-sec test pulse, and the recovery time course was identical in the WT and YAI mutant channels (Fig. 6B, *inset*). The mean recovery time course at −60 mV was best fit with two exponentials with time constants of 257 msec and 7.9 sec and the fast time constant accounting for 64% of the recovery. Thus, during 1-sec depolarizations, these Ca^{2+} channels enter both fast and slow inactivated states.

In the presence of drug, Ca^{2+} channels bind blocking drugs and inactivate in parallel during the 1-sec conditioning pulse. To show the time course of recovery from depolarized drug block alone, the recovery of current in the presence of drug was divided by the recovery of current in the absence of drug. This correction is only approximate because it does not account for inactivated channels that have also bound drug, but the results are affected only during the first second of recovery (Fig. 6B, *inset*). In the presence of blocking drugs at the concentrations used, 80–100% of the channels were blocked at the end of the 1-sec conditioning pulse. Recovery of these drug-blocked channels at −60 mV was slowed compared with controls (Fig. 6), and this effect of drug binding was greater for WT channels than for YAI in each case. The recovery time courses (Fig. 6, A–C) indicated that drug dissociation from channels was biexponential. The fast component of recovery from drug block is indicated more clearly on the expanded time scale in Fig. 6, D–F. The fast time constant of recovery (τ_F) was similar for all channels and drugs (400–500 msec). The most significant differences were in the slow time constant of recovery (τ_S) and the fraction of channels that recovered with each time course [fast recovery fraction (f_F)]. WT channels recovered most slowly from block by D888 and D600 (τ_S = 13 and 27 sec and f_F = 7% and 10%) and fastest from block by verapamil (τ_S = 7 and f_F = 42%). YAI channels recovered more rapidly from block than WT channels and became relatively insensitive to the structure of the drug applied (D888, verapamil, and D600: τ_S = 7.7, 4.4, and 7.0 sec, and f_F = 65%, 72%, and 58%, respectively).

Because the rate of block during depolarizations was increased for verapamil and D600 in mutant YAI (Fig. 5D), the observed reduction in use-dependent block in this mutant (Fig. 4) must be due to the acceleration of recovery rate demonstrated here. Even for verapamil, which has the fastest recovery in WT channels, the slow phase of recovery must be responsible for the use-dependent block developing over 20 sec (Fig. 4). Acceleration of this slowly recovering component in mutant YAI substantially reduces use dependence.

Effects of single-residue mutations on the kinetics of depolarized drug block. Mean rates of block of Y1463A,

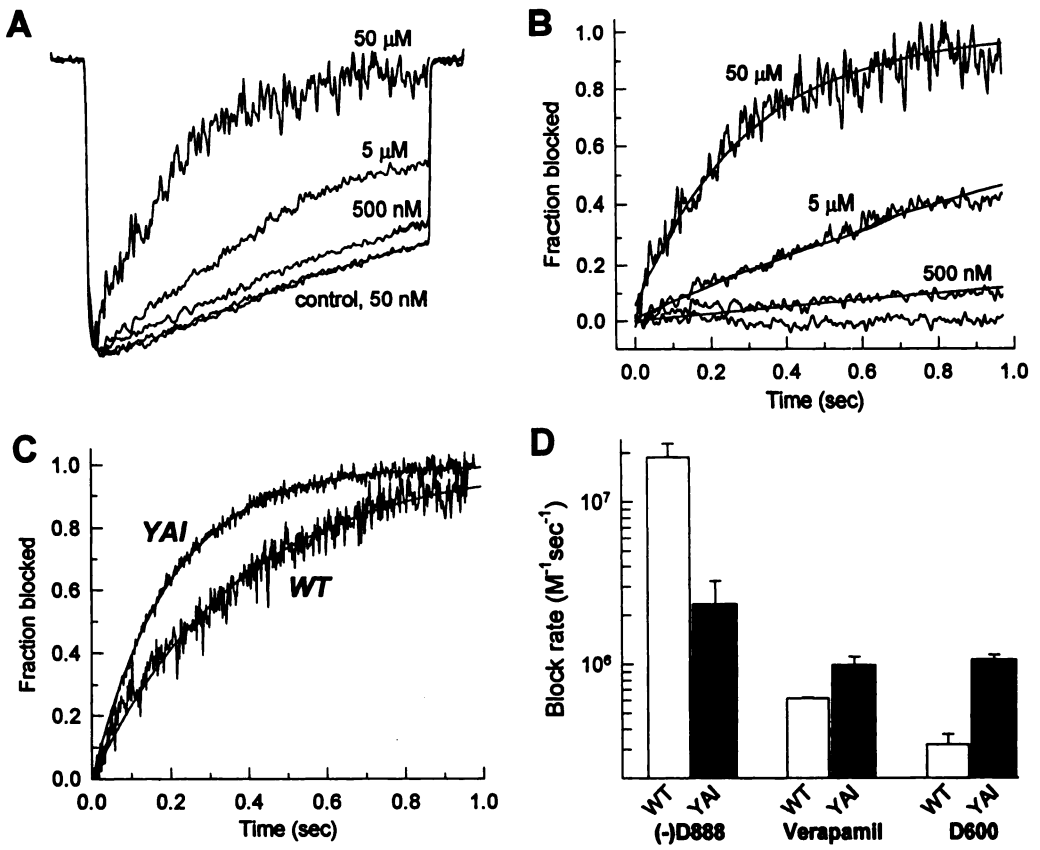

Fig. 5. Time course of block of depolarized channels. A, Currents from the cell shown in Fig. 1E (D600 on cells expressing WT channels) are scaled to permit comparison of current time course as D600 concentration is increased. The ratios of these scaled currents to current measured in the absence of drug (control) are shown in B with superimposed single-exponential fits (*smooth lines*). Time constants for these fits were 7.7 sec, 500 nM; 1.6 sec, 5 μM; and 310 msec, 50 μM. C, Mean time course of depolarized block by 5 μM D600 at +10 mV is compared in cells expressing WT and YAI channels. *Smooth lines*, single-exponential fits to the mean time courses with time constants of 375 msec (WT channels, $n = 3$) and 200 msec (YAI channels, $n = 3$). The data have been normalized according to the fit time constants. D, Mean block rates for each drug are compared for cells expressing WT and YAI channels (mean ± standard error, $n = 3$ or 4). Block rates were calculated by multiplying the inverse of the current decay time constant during the 1-sec depolarization to +10 mV by the inverse of the drug dose applied (50 nM for (−)-D888 on WT, 5 μM for all others).

A1467S, and I1470A by (−)-D888 were decreased 4.8–7.0-fold, similar to the 8-fold decrease observed for YAI (Fig. 7A). In contrast, the mutations of individual amino acid residues had quite different effects on the rate of block by verapamil. Y1463A increased the rate of block, whereas A1467S had little effect and I1470A decreased the rate of block. Therefore, the modest increase in the rate of block by verapamil in YAI is the net result of Y1463A increasing the rate of block and I1470A decreasing it.

The two time constants for recovery from drug block by (−)-D888 are affected little by the mutations A1467S and I1470A (Fig. 7B, *top*). However, the slow time constant of recovery from block by (−)-D888 is decreased and the fraction of fast recovery is substantially increased for Y1463A, as they are for YAI (Fig. 7B). For verapamil, none of the three single mutations had a significant effect on recovery rate or fast recovery fraction, which is consistent with the conclusion that the three mutated residues act in a concerted manner in determining the kinetics of verapamil dissociation in the combination mutant YAI.

Because the mutation Y1463A had the most substantial effects on the rate and affinity of drug binding, we studied the effects of other amino acid substitutions at this position. Different effects of Y1463F and Y1463T were observed for the rate of block at +10 mV and the recovery from block at −60 mV (Fig. 7, C and D). The block rate for (−)-D888 was reduced equally by both Y1463T and Y1463F but was reduced more by Y1463A (Fig. 7C), suggesting critical roles for both the hydroxyl group and phenyl ring of Y1463 in determining the rate of association of (−)-D888. In contrast to (−)-D888, Y1463F, Y1463T and Y1463A all increased the rate of association of verapamil (Fig. 7C).

These single mutations also had diverse effects on recovery rates. Y1463T increased the proportion of the fast phase of recovery from block by (−)-D888 ~10-fold, which is similar to Y1463A, but Y1463F had no effect on recovery. This suggests that the size and hydrophobicity of the residue at position 1463 are more important in determining the fast recovery from block by (−)-D888 at depolarized potentials than is interaction with the hydroxyl group. Individual substitutions for Y1463 had less marked effects on the increased rate of recovery from verapamil block observed with YAI (Fig. 7, B and D). Y1463A and Y1463T increased the fraction of fast recovery, whereas Y1463F reduced it. Thus, for verapamil, both the hydroxyl and the phenyl ring of Y1463 affect the time course of recovery from block.

Discussion

Two effects of mutations in IVS6 on block by phenylalkylamines. The three phenylalkylamines that were tested differ greatly in the characteristics of their block of L-type Ca^{2+} channels. Of the three, (−)-D888 is the most potent blocker of resting and depolarized L-type Ca^{2+} channels. Verapamil and D600 are less potent than (−)-D888 but are effective use-dependent blockers of WT channels.

Mutation of three amino acid residues in region IVS6 that differ between L- and N-type Ca^{2+} channels reduced block of resting L-type Ca^{2+} channels by (−)-D888 (10). The same mutations also reduced affinity of the depolarized Ca^{2+} channel for (−)-D888 indicating a reduction in affinity for drug binding to the open and inactivated states of the channel. Surprisingly, these mutations had no major effects on affinity for tonic block by D600 or verapamil. The disruption of

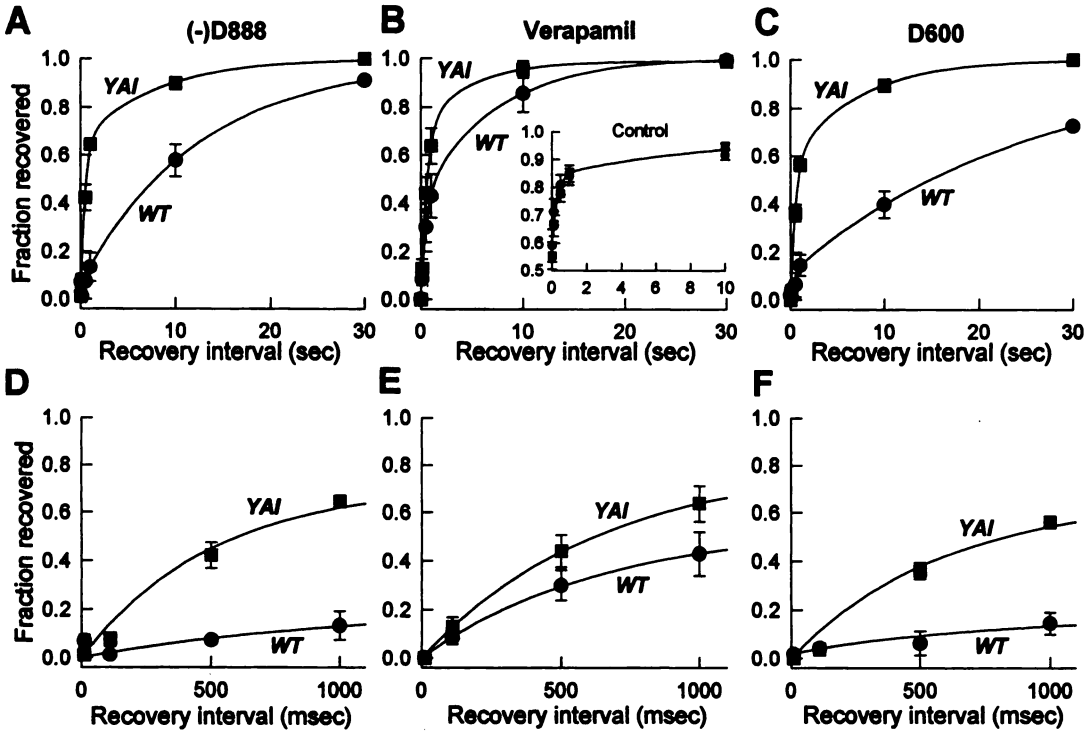

Fig. 6. Time course of recovery from depolarized channel block. Conditioning depolarizations to +10 mV for 1 sec were followed by recovery intervals (at −60 mV) of 10 msec, 110 msec, 500 msec, 1 sec, 10 sec, or 30 sec. A 100-msec test depolarization to +10 mV was then applied after each interval to measure recovery. The time course of recovery from drug-induced block was obtained by dividing the time course measured in the presence of drug by the time course measured in the absence of drug (B, *inset*). Mean fraction of current recovered is shown on two scales: 0–30 sec (A–C) and 0–1 sec (D–F). (−)-D888 (50 nM) was applied to cells expressing WT channels and 5 μM drug was applied to all others (n = 3–8). *Solid lines*, double-exponential fits to the mean data with a fast time constant (τ_F), slow time constant (τ_S), and fraction of channels recovering with the fast time constant (f_F). These values for D888 on cells expressing WT channels were τ_F = 0.47 sec, τ_S = 12.6 sec, and f_F = 6.7%; for YAI, τ_F = 0.47, τ_S = 7.7, and f_F = 65%; for verapamil on cells expressing WT channels, τ_F = 0.52, τ_S = 7.1, and f_F = 42%; for YAI, τ_F = 0.58, τ_S = 4.7, and f_F = 72%; for D600 on cells expressing WT channels, τ_F = 0.54, τ_S = 26.5, and f_F = 9.7%; and for YAI, τ_F = 0.53, τ_S = 7, and f_F = 58%. For the mean rate of recovery in the absence of drug (B, *inset*), τ_F = 0.26 sec, τ_S = 7.9 sec, and f_F = 64%.

block by (−)-D888 was highly structurally specific because mutation Y1463F, which removes only a single hydroxyl group at position 1463, resulted in a large disruption of block. Apparently, interaction of (−)-D888 with this single hydroxyl group accounts for much of the increased affinity of (−)-D888 relative to verapamil and D600.

The same mutations affected the rate at which all of the drugs blocked depolarized channels and the rate of recovery from block at the holding potential between depolarizations. Recovery at −60 mV was accelerated by the mutations comprising YAI for all three drugs. The effect was most dramatic for D600 and (−)-D888, drugs that caused the most slowly recovering block of the WT channel. Block of the channel by D600 and verapamil was also accelerated by the YAI mutation. This effect was not seen for block by (−)-D888, but it was likely to have been counteracted by the large decrease in affinity of the mutant channel for this drug. These results suggest that these three mutations alter both affinity for and drug access to the phenylalkylamine-binding site.

A kinetic model for Ca^{2+} channel block by phenylalkylamines. To separate the effects of our mutations on affinity and drug access more clearly and to understand how the observed changes in use-dependent block and recovery time course might come about, a kinetic model of drug interaction with three primary channel states was constructed (see Materials and Methods) and used to reproduce the data (Fig. 8) with the constraints described and the parameters listed in Tables 1 and 2. A schematic diagram of this model is shown in Fig. 8D (*inset*). Drug is assumed to bind and block closed, open, and inactivated channels without preventing transitions between each of the elementary channel states (e.g., closed blocked channels can become open blocked channels, and so on). This was the simplest model that would describe our data. It reproduced the observed results for: 1) channel behavior in the absence of drug (Figs. 1, C–E, 6B, *inset*, and 8A), 2) tonic block of resting channels at −60 mV and depolarized channels at +10 mV (Figs. 1, C–E, 2, and 8, A, C, and E), 3) the apparent block rate of depolarized channels (Figs. 5, and 8, A, C, and E), and 4) the biexponential time course of recovery from depolarized drug block (Figs. 6, 8, B, D, and F, and 9B).

According to the model, the channel opens on depolarization (state O) and then sequentially enters two inactivated states: I1 and I2. Two inactivated states were required to fit the biexponential recovery from inactivation after a 1-sec depolarization to +10 mV in the absence of drug (Fig. 6B, *inset*). Control current time courses were identical for the WT and mutant YAI channels; the mean is shown in Fig. 8A (*dashed line superimposed on the model fit*). Recovery time courses for WT and YAI channels under control conditions were also identical, as shown in Fig. 6B (*inset*). Each of these comparisons between the experimental data and the predictions of the model resulted in a close fit.

Our experiments demonstrate that drug binds to both rest-

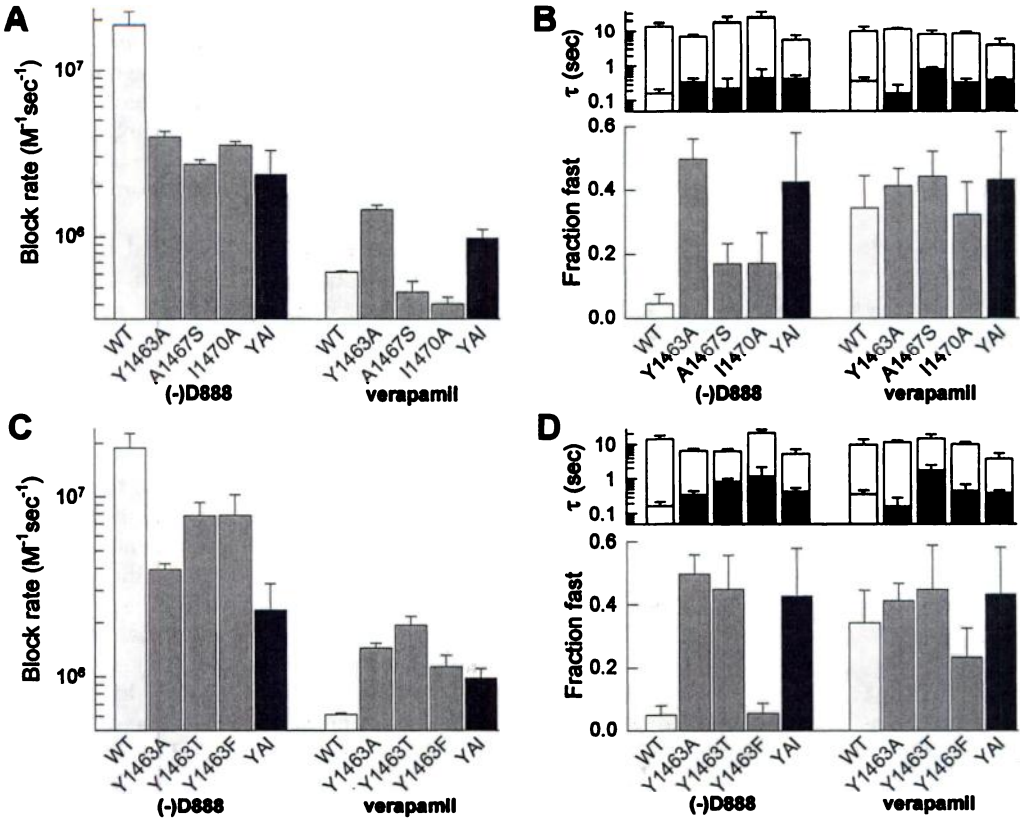

Fig. 7. Effect of individual amino acid substitutions on the time course of phenylalkylamine block. The individual mutations constituting the mutant YAI, Y1463A, A1467S, and I1470A and substitutions of phenylalanine (F) and threonine (T) for the tyrosine at position 1463 were characterized as shown in previous figure legends. A and C, Mean block rates (n = 3–6 for single mutants). B and D, Mean recovery time courses (n = 3–8 for single mutants). Recovery time courses were fit with the sum of two exponentials. Both time constants and the fraction recovering with the fast time constant are shown. (−)-D888 was applied over a concentration range of 5 nM to 50 μM, and verapamil was applied over a range of 500 nM to 50 μM.

ing and depolarized states of the channel but with different affinities. Transition rates between drug-bound states for the three drugs tested were set to simulate the degree of resting channel block (Fig. 2B), the magnitude of depolarization-induced drug block (Fig. 2C), and time course of recovery from depolarized drug block (Fig. 9B) obtained from the mean values shown in the figures. The biexponential time course of recovery from depolarized block was seen most prominently in WT channels for block by verapamil but was seen in the YAI mutant for block by all three drugs (Fig. 6). In the model, the rapidly recovering component arises from drug-bound open channels that are blocked during the depolarization. The slowly recovering component results from drug-bound inactivated channels. In the WT channel, the slow recovery from block by (−)-D888 and D600 was also predominantly caused by a slow rate of recovery of drug-bound, inactivated channels.

The increase in the fraction of channels found in the fast recovering state (open blocked channels) in YAI compared with WT channels arose from a decrease in the affinity of the inactivated state for all three drugs (Table 2). The drug affinity for the inactivated channel decreased 355-fold for D888 (K_d = 1.21 nM in WT channels versus 429 nM in YAI channels), decreased only 3.2-fold for verapamil (K_d = 200 nM in WT channels versus 643 nM in YAI channels), and decreased 17.8-fold for D600 (K_d = 19.3 nM in WT channels to 343 nM in YAI channels).

The increases in block rates for verapamil and D600 for mutant YAI, which occur without changes in apparent affinity for depolarized channels, arise from increases in access to

TABLE 2

Rate constants and K_d values of drug-blocked channel states used in the kinetic model

Mean data for WT and YAI channel recovery from depolarized drug block (Fig. 9B) were fit using the kinetic scheme diagrammed in Fig. 8D (*inset*). Block of inactivated channels in both states, I_1B and I_2B, were set to be equal (see Materials and Methods). The behavior of the model using these rate constants is shown in Fig. 8 as solid lines during depolarizations to +10 mV and as recovery time course at −60 mV.

	D888			Verapamil			D600		
	k_{on}	k_{off}	K_d	k_{on}	k_{off}	K_d	k_{on}	k_{off}	K_d
	$M^{-1}\ sec^{-1}$	sec^{-1}	nM	$M^{-1}\ sec^{-1}$	sec^{-1}	nM	$M^{-1}\ sec^{-1}$	sec^{-1}	nM
CB									
WT	1,000	4.8×10^{-5}	48	1,000	6.7×10^{-3}	6,700	1,000	9×10^{-3}	9,000
YAI	1,000	500×10^{-5}	5,000	1,000	6.0×10^{-3}	6,000	1,000	13×10^{-3}	13,000
OB									
WT	1.8×10^7	0.03	1.67	9.6×10^5	0.35	365	2.4×10^5	0.12	500
YAI	1.2×10^6	0.45	375	1.7×10^6	0.6	353	1.8×10^6	1.5	833
IB									
WT	1.4×10^9	1.7	1.21	1.4×10^7	2.8	200	1.4×10^7	0.27	19.3
YAI	1.4×10^7	6.0	429	1.4×10^7	9.0	643	1.4×10^7	4.8	343

CB, block of closed channel; OB, block of open channel; IB block of inactivated channels.

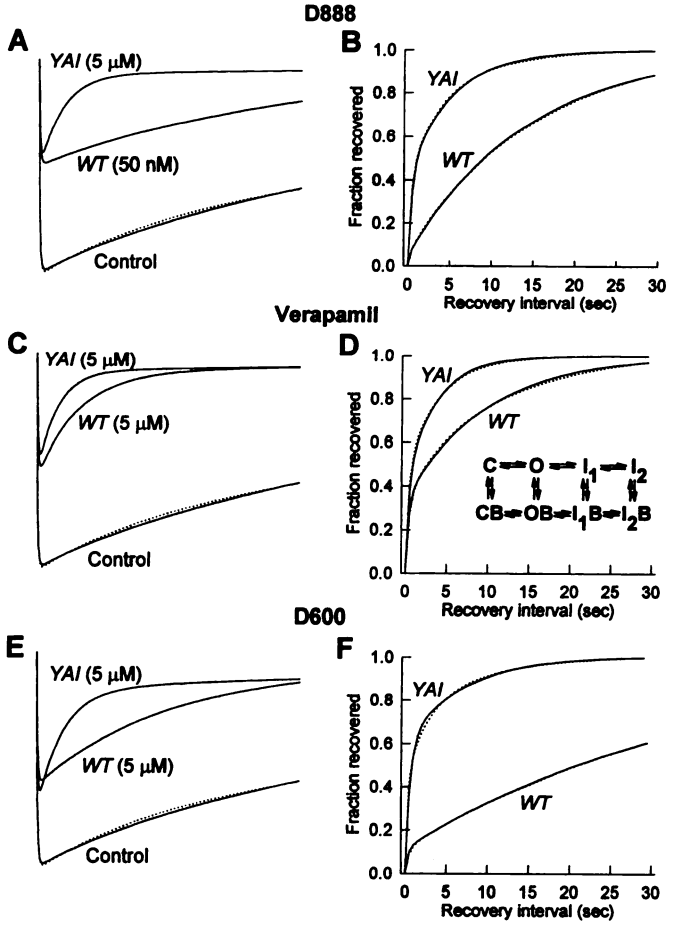

Fig. 8. State-dependent model of Ca^{2+} channel block by phenylalkylamines. Predicted current traces (*solid lines*) are illustrated for a kinetic model of channel block by phenylalkylamines of the form shown in D (*inset*) with the best-fit parameters listed in Tables 1 and 2 and are compared with experimentally determined values (*dashed lines*). The model was first fit to mean experimentally determined channel activation and inactivation (A, C, and E; *dashed lines*), deactivation, and recovery from inactivation (Fig. 6B, *inset*) measured in the absence of drug and then fit to mean recovery from depolarized drug block (B, D, and F; dashed lines) for each of the three drugs and both WT and YAI channels (Figs. 6 and 9B). The magnitude and time course of the calculated currents evoked during a 1-sec depolarization in the presence of drug (A, C, and E) were then plotted to compare the model behavior with that measured under each condition (Fig. 1, C–E). Apparent block rates calculated from this simulated data are similar to mean data summarized in Fig. 5D (D888: WT channel = 2.2×10^7 M^{-1} sec^{-1}, YAI = 2.3×10^6; verapamil: WT channel = 1.3×10^6, YAI = 2.7×10^6; D600: WT channel = 4.5×10^5, YAI = 2.1×10^6). Rate constants derived for each of the channel states are summarized in Materials and Methods and Tables 1 and 2.

the open blocked state and compensating increases in dissociation from this channel state. This was seen in the model as an increase in the association rate for drug block of open channels of 1.8-fold for verapamil and 7.5-fold for D600 (Table 2). A decrease in the affinity of the inactivated state of the channel for drug is seen as a reduction in the number of channels that recover slowly and a speeding of the time course of this slow recovery (Fig. 6) but not as a change in the apparent depolarized affinity (Fig. 2C).

Three amino acids determine the high affinity of L-type channels for (−)-D888. The high affinity blocker (−)-D888 has only a single methoxy group in the *meta* position of the phenyl ring nearest the amine, whereas D600 and verapamil have one in the *meta* and one in the *para* position (Fig. 1A). The second methoxy group on this end of the phenylalkylamine molecule has a negative influence on phenylalkylamine action (22). Thus, the single methoxy group on (−)-D888 is expected to have a more effective interaction with the channel than the corresponding group in the other phenylalkylamines.

Our results indicate that each of the individual amino acid side chains of the YAI residues participates in stabilizing (−)-D888 in its binding site. For resting block, each of the amino acid side chains contributes approximately equally in stabilizing (−)-D888, but the disruption caused by each individual mutation is greater than would be expected if each of the amino acids constituting mutation YAI interacted independently with the drug. This is even more striking for block of depolarized channels because mutating any of the individual amino acids causes near total disruption of block observed after mutation of all three of the amino acids constituting YAI. This suggests that these three amino acids are required to form a structure that stabilizes the drug optimally in its binding site and that all must be present to stabilize the bound drug at depolarized potentials.

Mutations constituting YAI define the kinetics of drug block. The kinetics of block by each of the drugs were affected by the mutations constituting YAI. Despite the lack of effect of these mutations on the affinity for resting and depolarized channels, the rate of block by verapamil and D600 during depolarizations and the rate of block reversal for all drugs were dramatically affected by this combined mutation. These effects are consistent with effects of these mutations both on a rate-limiting access pathway for drug entry and exit from the binding site and on the affinity of inactivated channels for drug. Mutations affecting both drug affinity and drug access have also been identified for local anesthetics binding to a site on the IVS6 transmembrane segment of Na^+ channels (23).

Like the effects on affinity, the effects on blocking kinetics involved all three residues. Block rate by D888 was reduced by mutation of all three residues. Verapamil block rate was increased by mutations Y1463A, Y1463T, and Y1463F but reduced slightly by A1467S and I1470A. The acceleration of recovery from depolarized block by (−)-D888 could be almost entirely attributed to Y1463A, with little effect observed for the A1467S or I1470A mutations. Consistent with the hypothesis that the size and shape of the residue at position 1463 control the pathway by which D888 leaves its binding site, mutation Y1463T had effects that were similar to those of Y1463A, whereas mutation Y1463F had recovery kinetics that were essentially WT.

Molecular model of Ca^{2+} channel block by phenylalkylamines. Fig. 1A shows the structures of D888, verapamil, and D600. When data from control and YAI channels from previous figures are summarized with respect to the total number and position of methoxy groups on the phenylalkylamine molecules, the effect of each methoxy group on channel block becomes evident (Fig. 9). In Fig. 9A, the block rates for each compound are arranged in order of ascending number of methoxy groups on the two phenyl rings. On adding a methoxy group to D888 in the *para* position of one phenyl ring to yield verapamil, block rate drops by 31-fold in the WT channel. On adding a methoxy group to the other end of the

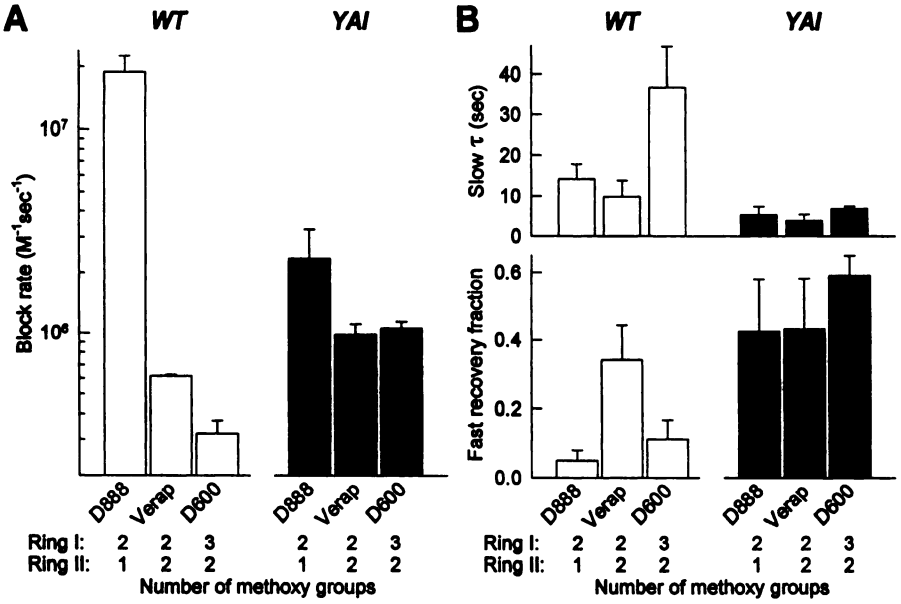

Fig. 9. Structure-block relation for three phenylalkylamines. Block rates (A) and recovery time courses (B) for WT and YAI channels are shown as a function of the number and position of methoxy groups on both phenyl rings of the phenylalkylamines (see Fig. 1A for structures). D888 has two methoxy groups on the primary phenyl ring and one on the secondary ring; verapamil has two on the primary phenyl ring and two on the secondary ring; and D600 has three on the primary phenyl ring and two on the secondary ring. Data are summarized from previous figures.

molecule in the *meta* position to yield D600, block rate decreases an additional 2-fold. For the same changes in drug structure, comparatively little alteration in block rate occurs for the mutant YAI, and both D888 and D600 block the channel more like verapamil. In looking at recovery time courses (Fig. 9B), it is apparent that the addition of a methoxy group to D888 to give verapamil results in an increase in the fraction of fast recovery, whereas the addition of another methoxy group to the other phenyl ring of verapamil to yield D600 results in both a decrease in the fraction of fast recovery and an increase in the slow recovery time constant. Regarding association rates, the same changes in the drug molecule lead to statistically insignificant differences in block of the mutant YAI.

These results can be interpreted in terms of both crystal structures and calculated structures of phenylalkylamines, which indicate that these molecules are bent with both phenyl rings pointing in the same direction (24–27). The YAI mutations affect block by these compounds differently, suggesting interactions with both ends of the drug. In studies of drug structure and cardiac function (22), the results suggested that the addition of a methoxy group in the *para* position (e.g., D888 to verapamil) leads to reduced effectiveness through steric hindrance. Our data suggest that the YAI residues both interact directly with the bound drug and introduce steric hindrance to drug access and binding. The critical role of Y1463 in resting block of (−)-D888 shown in our previous study (10) suggests that it constitutes one point in a two-member binding motif on transmembrane segment IVS6, whereas A1470 and I1473 constitute the other half. The addition of a methoxy group to the *para* position may introduce steric hindrance through an interaction with the bulky side chain on the Y1463 phenyl ring. The addition of another methoxy group on the other end of the phenylalkylamine to yield D600 apparently adds another point of steric hindrance that slows both block rate and recovery rate by making it more difficult to enter the binding site. Further analysis of the effect of the other nearby amino acid residues will be required to define the positions of the bound drug molecule in its receptor site, but we assume that the positively charged amino group approaches and interacts with the negatively charged residues in the ion selectivity filter formed by SS1/SS2 (or P) loop and also interacts with Y1463 in the phenylalkylamine receptor site.

References

1. Fleckenstein, A., and G. Fleckenstein-Grun. Cardiovascular protection by Ca^{2+} antagonists. *Eur. Heart J.* **1**:15–21 (1980).
2. Catterall, W. A. Structure and function of voltage-gated ion channels. *Annu. Rev. Biochem.* **64**:493–531 (1995).
3. Hofmann, F., M. Biel, and V. Flockerzi. Molecular basis for Ca^{2+} channel diversity. *Annu. Rev. Neurosci.* **17**:399–418 (1994).
4. Glossmann, H., and J. Striessnig. Molecular properties of Ca^{2+} channels. *Rev. Physiol. Biochem. Pharmacol.* **114**:1–105 (1990).
5. Lee, K. S., and R. W. Tsien. Mechanism of calcium channel blockade by verapamil, D600, diltiazem and nitrendipine in single dialysed heart cells. *Nature (Lond.)* **302**:790–794 (1983).
6. Hescheler, J., G. Pelzer, G. Trube, and W. Trautwein. Does the organic calcium channel blocker D600 act from inside or outside of the cell membrane? *Pflueg. Arch. Eur. J. Physiol.* **393**:287–291 (1982).
7. Hille, B. Local anesthetics: hydrophilic and hydrophobic pathways for the drug-receptor reaction. *J. Gen. Physiol.* **69**:497–515 (1977).
8. Striessnig, J., H.-G. Knaus, M. Grabner, K. Moosburger, W. Seitz, H. Lietz, and H. Glossmann. Photoaffinity labeling of the phenylalkylamine receptor of the skeletal muscle transverse-tubule calcium channel. *FEBS Lett.* **212**:247–253 (1987).
9. Striessnig, J., H. Glossmann, and W. A. Catterall. Identification of a phenylalkylamine binding region within the $\alpha 1$ subunit of skeletal muscle Ca^{2+} channels. *Proc. Natl. Acad. Sci. USA* **87**:9108–9112 (1990).
10. Hockerman, G. H., B. D. Johnson, T. Scheuer, and W. A. Catterall. Molecular determinants of high affinity phenylalkylamine block of L-type calcium channels. *J. Biol. Chem.* **270**:22119–22122 (1995).
11. Schuster, A., L. Lacinová, N. Klugbauer, H. Ito, L. Birnbaumer, and F. Hofmann. The IVS6 segment of the L-type calcium channel is critical for the action of dihydropyridines and phenylalkylamines. *EMBO J.* **15**:2365–2370 (1996).
12. Döring, F., V. E. Degtiar, M. Grabner, J. Striessnig, S. Hering, and H. Glossmann. Transfer of L-type calcium channel IVS6 segment increases phenylalkylamine sensitivity of α_{1A}. *J. Biol. Chem.* **271**:11745–11749 (1996).
13. Kunkel, T. A. Rapid and efficient site-specific mutagenesis without phenotypic selection. *Proc. Natl. Acad. Sci. USA* **82**:488–492 (1985).
14. Snutch, T. P., W. J. Tomlinson, J. P. Leonard, and M. M. Gilbert. Distinct calcium channels are generated by alternative splicing and are differentially expressed in the mammalian CNS. *Neuron* **7**:45–57 (1991).
15. Pragnell, M., J. Sakamoto, S. D. Jay, and K. P. Campbell. Cloning and tissue-specific expression of the brain calcium channel β-subunit. *FEBS Lett.* **291**:253–258 (1991).
16. Ellis, S. B., M. E. Williams, N. R. Ways, R. Brenner, A. H. Sharp, A. T. Leung, K. P. Campbell, E. McKenna, W. J. Koch, A. Hui, A. Schwartz, and M. M. Harpold. Sequence and expression of mRNAs encoding the $\alpha 1$ and $\alpha 2$ subunits of a DHP-sensitive calcium channel. *Science (Washington D. C.)* **241**:1661–1664 (1988).
17. Margolskee, R. F., B. McHendry-Rinde, and R. Horn. Panning transfected cells for electrophysiological studies. *Biotechniques* **15**:906–911 (1994).

18. Mannhold, R., R. Bayer, M. Ronsdorf, and L. Martens. Comparative QSAR studies on vasodilatory and negative inotropic properties of ring-varied verapamil congeners. *Arzneim. Forsch.* **37**:419–424 (1987).
19. Ferry, D. R., H. Glossmann, and A. J. Kaumann. Relationship between the stereoselective negative inotropic effects of verapamil enantiomers and their binding to putative calcium channels in human heart. *Br. J. Pharmacol.* **84**:811–824 (1985).
20. Courtney, K. R., J. J. Kendig, and E. M. Cohen. The rate of interaction of local anesthetics with sodium channels in nerve. *J. Pharmacol. Exp. Ther.* **207**:594–604.
21. Timin, E. N., and S. Hering. A method for estimation of drug affinity constants to the open conformational state of calcium channels. *Biophys. J.* **63**:808–814 (1992).
22. Mannhold, R. Molecular pharmacology of calcium antagonists, in *Recent Advances in Receptor Chemistry* (C. Melchiorre and M. Giannella, eds.). Elsevier Science Publishers, Amsterdam, 147–171 (1988).
23. Ragsdale, D. S., J. C. McPhee, T. Scheuer, and W. A. Catterall. Molecular determinants of state-dependent block of Na^+ channels by local anesthetics. *Science (Washington D. C.)* **265**:1724–1728 (1994).
24. Dei, S., M. N. Romanelli, S. Scapecchi, E. Teodori, A. Chiarini, and F. Gualtieri. Verapamil analogues with restricted molecular flexibility. *J. Med. Chem.* **34**:2219–2225 (1991).
25. Zhorov, B. S. Comparison of lowest energy conformations of dimethylcurine and methoxyverapamil: evidence of ternary association of calcium channel, Ca^{2+}, and calcium entry blockers. *J. Membr. Biol.* **133**:119–127 (1993).
26. Carpy, A., and J.-M. Léger. Structure of α-isopropyl-α-[(N-methyl-N-homoveratryl)-γ-aminopropyl]-3,4-dimethoxyphenylacetonitrile hydrochloride, verapamil, $C_{27}H_{38}N_2O_4$. HCL. *Acta Crystallogr. Sect. C Cryst. Struct. Commun.* **41**:624–627 (1985).
27. Brasseur, R., M. Deleers, and W. J. Malaisse. Conformational analysis of the calcium antagonist gallopamil. *Biochem. Pharmacol.* **32**:437–440 (1983).

Send reprint requests to: Dr. William A. Catterall, Department of Pharmacology, Box 357280, University of Washington School of Medicine, Seattle, WA 98195-7280. E-mail: wcatt@u.washington.edu